MORPHOMETRIC DATA ON THE ENDOTHELIUM OF BLOOD CAPILLARIES

MAIA SIMIONESCU, NICOLAE SIMIONESCU, and GEORGE E. PALADE

From The Rockefeller University, New York 10021. Doctors M. and N. Simionescu's permanent address is The Institute of Endocrinology, Bucharest, Romania.

ABSTRACT

Local differentiations within the endothelium of both muscular (diaphragm, myocardium) and visceral (pancreas, jejunal villi) capillaries have been studied in rats on sectioned and freeze-cleaved preparations. Four distinct parts have been recognized in the endothelial cells of all these vessels on the basis of subcellular components present in each part and on the basis of variations in the local frequency of plasmalemmal vesicles: (*a*) the parajunctional zone, (*b*) the peripheral zone, (*c*) the organelle region, and (*d*) the nuclear region. Our data indicate that ~16, ~7.0, and 8.5% of the endothelial cytoplasmic volume (in the peripheral zone) is accounted for by vesicles, their content, and their membranes, respectively. The average density of vesicular openings per μm^2 is 78 in diaphragm, 89 in myocardium, 25 in pancreas, and 10 in jejunal mucosa capillaries. The frequency of fenestrae is 1.7 times as high in jejunal ($26/\mu m^2$) as in pancreatic capillaries ($15/\mu m^2$), the corresponding fractional areas being ~9.5 and ~6%, respectively, of the endothelial surface. Intercellular spaces occupy a relatively small area (~0.08 to 0.2%) of the inner endothelial surface.

INTRODUCTION

Previous studies have shown that the endothelial layer of both muscular and visceral capillaries is heterogeneous in its organization, primarily on account of an uneven distribution of various subcellular structures (1, 2). Among the latter, the plasmalemmal vesicles in the endothelium of muscular capillaries and the fenestrae in that of visceral capillaries are of particular importance, since they have been implicated in the movement of water and water-soluble molecules across the endothelial layer (2, 3–8). A number of incidental observations have already mentioned an uneven distribution of fenestrae and vesicles in a variety of capillaries (6, 9–19). Moreover, in a recent paper (8) we have distinguished in the endothelial cell of the blood capillaries of the rat diaphragm four differentiated parts, and we have shown that these parts participate unequally in the transport of myoglobin used as an exogenous tracer. But more extensive observations and more precise morphometric data on the general structure and local differentiations of the endothelium are needed for an adequate structural interpretation of physiological findings on capillary permeability. In this paper we present a series of observations on local differentiations within the endothelium of both muscular (diaphragm, myocardium) and visceral (pancreas, intestinal mucosa) capillaries. The data have been obtained on sectioned as well as on freeze-cleaved preparations.

MATERIALS AND METHODS

Animals

For these observations we used 46 young adult rats of the Wistar-Furth and Sprague-Dawley strains. The animals were lightly anesthetized with ether to allow fixation *in situ* before collection of tissue specimens (1, 2).

Tissue Preparation

Fixation was carried out *in situ* as indicated in reference 1 for diaphragm and heart, and in reference 7 for jejunum. Pancreatic lobules were fixed by injecting the fixative directly into the perilobular loose connective tissue, the rest of the preparation procedure being the same as for the diaphragm.

SECTIONED SPECIMENS: Diaphragm specimens were processed for conventional electron microscopy by using the fixative mixture and general procedure given in reference 7.

FREEZE-CLEAVAGE: After a 5-min fixation *in situ* with 3% glutaraldehyde in 0.1 M HCl-Na cacodylate buffer, pH 7.2, tissue blocks of ~0.5 × 0.5 × 0.25 mm in size were transferred to the same fixative solution for 20 min and then immersed for 2 h in either glycerol (25% in 0.1 M HCl-Na cacodylate buffer, pH 7.2) or sucrose (25% in 0.1 M phosphate buffer, pH 7.2). Blocks treated in this way were mounted on cardboard discs, quickly frozen in liquid Freon 22 (chlorodifluoromethane), and fractured in a Balzers apparatus (Balzers A. G., Balzers, Lichtenstein) at a pressure of 2×10^{-6} Torr and a stage temperature of −115°C (20, 21). The cleaved surfaces were replicated with platinum-carbon, and the replicas were cleaned with a 15% sodium hypochlorite solution, mounted on uncoated 300-mesh grids, and finally examined in a Philips EM 300 electron microscope operated at 80 kV and provided with apertures of 200 m (diameter) in the condenser and 30 μm in the objective lens. The instrument was calibrated with a cross-lined carbon grating replica (2160 lines per mm).

Morphometry

Measurements were made on appropriately enlarged electron micrographs using a calibrated 7× magnifier, a Keuffel and Esser planimeter, and a map measure. In the case of replicas, the regions used were carefully selected in favor of flat, horizontal surfaces.

Our present observations concern capillaries with the following average inner diameter diaphragm, 5 ± 1 μm; myocardium, 6.6 ± 1 μm; pancreas, 7.2 ± 1.8 μm; and jejunum, 8 ± 2.1 μm.

RESULTS

Sectioned Specimens

Sectioned specimens have been used to obtain volume-related parameters. The inquiry has been limited to the capillaries of the diaphragm and represents an extension of the work already presented in reference 8.

The examination of a large number of micrographs in control and experimental animals (myoglobin experiments [8]) has indicated that four distinct parts can be recognized in any endothelial cell. Two of them are located at the cell's periphery, have the form of belts or coronas, and are referred to as zones, namely (*a*) the parajunctional zone, and (*b*) the peripheral zone. The two others represent central regions, namely, (*c*) the organelle region and (*d*) the nuclear regions (Fig. 1).

Table I gives the average thickness, average volume, and vesicle frequency per μm^3 in each of the four parts. A short description of the latter follows.

(*a*) *The parajunctional zone* is characterized by low frequency or absence of plasmalemmal vesicles; other subcellular components are also rare or absent. The limits of this zone are by necessity arbitrary and are set by points separating vesicle-free from vesicle-provided areas on each cell front. The volume of the zone is delimited by lines connecting these points across the endothelium (see Fig. 1). Within this zone, there are a few vesicles either free in the cytoplasmic matrix or open in the intercellular spaces, usually abluminally from the intercellular junctions.[1]

(*b*) *The peripheral zone* accounts for ~40% of the cell's cytoplasmic volume and, by its size and large vesicle population, appears to be functionally the most important part of the endothelial cell. Table I, which gives in addition to vesicle frequency the volume fraction taken by vesicles in each region, shows that the cell periphery is characterized by the highest fractional volumes accounted for by vesicles as well as by

[1] A survey of 251 capillary profiles (rat diaphragm) with a total number of 404 endothelial intercellular spaces showed that ~18% of the latter were provided with open vesicles. Vesicle frequency was about three times (~3 open vesicles) higher for the long (1–2 μm), oblique intercellular spaces than for the short (0.3–0.65 μm), straight intercellular spaces which usually had only one open vesicle.

vesicle content and membrane. In addition to plasmalemmal vesicles, the region contains, in small numbers, all the usual subcellular cytoplasmic components with the exception of the Golgi complex and centrioles.

(*c*) *The organelle region* is generally adjacent to the nucleus, but does not appear to surround it completely. This region has a high concentration of cytoplasmic organelles (mitochondria, endoplasmic reticulum, free and bound polysomes, microtubules, glycogen particles); accommodates the Golgi complex, the centrioles, and occasionally a few lysosomes; and is characterized by a relatively small vesicular population, ~4 times smaller than in the peripheral zone, or ~2 times lower, if the volume occupied by the organelle mass is subtracted from the total volume of the region.

(*d*) *The nuclear region* is occupied by the nucleus and a thin shell of cytoplasm around it usually devoid of cellular organelles. The perinuclear cytoplasm represents about ⅓ of the total cytoplasmic volume of the endothelial cell, and the vesicle frequency therein is only slightly lower than in the peripheral zone.

Considered together, the data in Table I indicate that ~11.1, ~5.1, and ~6.0% of the total cytoplasmic volume of the endothelium is accounted for by plasmalemmal vesicles, their content, and their membranes, respectively. The last figure shows that the endothelial cell has 4 times more membrane in plasmalemmal vesicles than in the plasmalemma proper (the latter represents ~1.6% of the cytoplasmic volume).

Freeze-Cleaved Specimens

Morphometric data on certain endothelial structures (plasmalemmal vesicles, fenestrae, intercellular spaces) can more easily be obtained by using the freeze-cleavage technique which exposes large intramembranous surface areas (cf. 21) on both endothelial fronts. Instances in which a membrane cleavage plane abuts against a cross fracture of the endothelium allow the identification of specialized surface features

---

General abbreviations used in legends:

A_b, A face (inner leaflet) of the endothelial plasma-lemma on the blood front
A_t, A face (inner leaflet) of the endothelial plasma-lemma on the tissue front
B_b, B face (outer leaflet) of the endothelial plasmalemma of the blood front
B_t, B face (outer leaflet) of the endothelial plasmalemma on the tissue front
bm, basement membrane
c, collagen fibrils
cr, craters (fenestrae or vesicular stomata on B faces)
e, endothelium
er, endoplasmic reticulum
f, fenestra
i, intercellular space in the endothelium
m, mitochondrion
mf, muscle fiber
n, nucleus
np, nuclear pores
nr, nuclear region
or, organelle region
p, particles, intramembranous
pc, pericyte
pd, pericyte pseudopod
pjz, parajunctional zone
pl, plasma
pn, perinuclear cytoplasm
pp, circumvallate papillae (fenestrae or vesicular stomata on A faces)
ps, pericapillary space
pz, peripheral zone
rbc, red blood cell
sv, sarcolemmal vesicle
v, plasmalemmal vesicle

All micrographs of freeze-fracture replicas are mounted with the shadows generally projecting from bottom to top; the exact shadowing direction is indicated by the arrow put on the number of each figure.

FIGURES 1 *a* and *b* Comparison between a section and a replica of a nearly transverse fracture through a blood capillary of rat diaphragm. The fracture exposes the B face of the plasmalemma on the tissue from at B_t and the A and B faces of the plasmalemma on the blood front at A_b and B_b, respectively. In both cases the four regions of the endothelial cells can be seen and are marked *pjz*, parajunctional zone; *pz*, peripheral zone; *or*, organelle region; and *nr*, nuclear region. Fig. 1 *a*: × 34,000; Fig. 1 *b*: × 31,000.

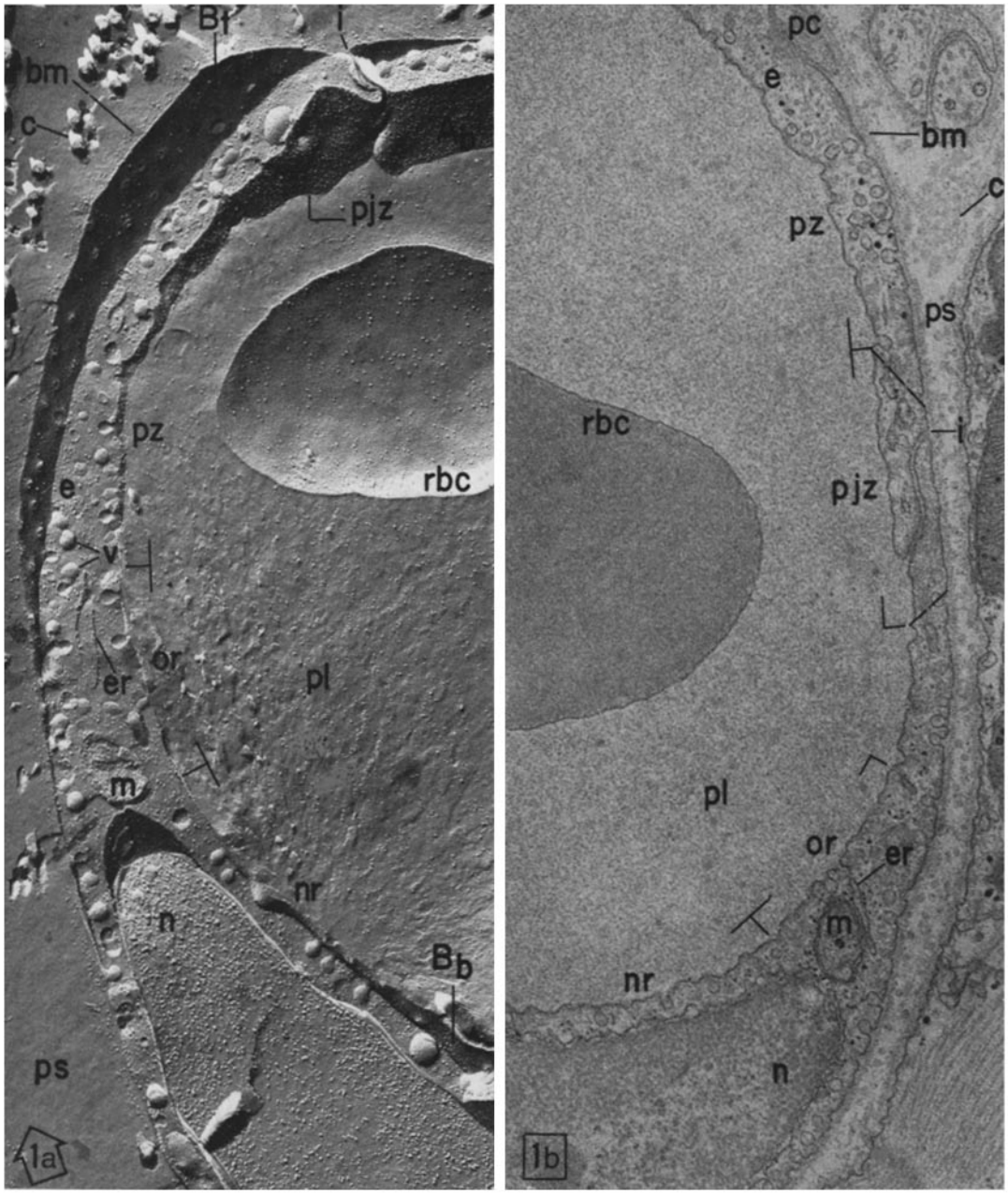
Bf
i
bm
c
pjz
pz
rbc
e
v
or
er
pl
m
nr
n
Bb
ps
1a
pc
e
bm
c
pz
ps
i
rbc
pjz
pl
or
er
m
nr
n
1b

TABLE I

Volume Distribution in the Endothelium of Diaphragm Capillaries (Rat)

Zones and regions	Average thickness*	Relative volume*	Plasmalemmal vesicles: Frequency‡/μm^3 cytoplasm (range)	Plasmalemmal vesicles: Average fractional volume§: Total‖	Mem-brane‖	Con-tent‖
	μm	%		%	%	%
Peripheral zone	0.25 ± 0.05	39 ± 6	875 (442–1310)	15.7	8.5	7.2
Organelle region	0.55 ± 0.09	18 ± 4	221 (144–308)	4.0	2.2	1.8
Nuclear region¶	2.1 ± 0.6	32 ± 4	709 (496–1216)	12.7	6.9	5.8
Parajunctional zone	0.18 ± 0.03	11 ± 3	57 (0–82)	1.0	0.6	0.4

* Measurements made on 72 capillary profiles with an aggregated endothelial volume of 10.79 μm^3 (estimated by assuming an average section thickness of 600 Å).

‡ The total number of vesicles counted was 6658 on 38 capillary profiles of ~5 to 7 μm diameter.

§ Calculated by assuming for all vesicles, closed or open, the following dimensions: outer diameter = 700 Å; inner diameter = 540 Å; mean thickness of vesicular membranes = 80 Å.

‖ Percentage of the endothelial volume per zone.

¶ Nucleus excluded from all values except average thickness.

belonging to the A face or B face of the plasmalemma on each cell front.

To obtain more information on both muscle and visceral types of capillaries, the investigation was extended to two tissue specimens for each category, namely diaphragm and myocardium for the first and pancreas and jejunal mucosa for the second.

General Observations

For all types of small vessels examined, the cleavage plane passes preferentially along the tissue front of the endothelium and more rarely along its blood front. Both faces are marked by randomly distributed particles of 9–15 nm diameter (measured without correction for metal shadowing). The ones on the A faces are generally larger and 4–6 times more numerous than those on the B faces, but their frequency varies considerably (from 100 to 800 particles per μm^2) from region to region (Figs. 2 and 3). These particles appear to be the endothelial equivalent of the intramembranous particles described in other membranes (21, 22). Their general distribution on the cleavage faces is comparable to that recorded in other cell types, but the frequency of large particles (diameter $\simeq$ 15 nm) is higher.

Besides particles, the cleavage surfaces are marked by crater-like and papilla-like structures, the first preferentially found on B faces (Figs. 2, 3, and 15 a) and the latter on A faces (Figs. 2, 3, and 6). As will be shown later on, these features represent either fenestrae or vesicular stomata. Particles of the dimensions mentioned are rarely seen on either craters or papillae (Figs. 2 and 6 a, b).

Since on cleaved membranes only the parajunctional zones can be recognized with certainty, the description that follows applies to the three other endothelial regions taken together.

Plasmalemmal Vesicles

STRUCTURAL ASPECTS: In all capillaries examined, we have found craters with elevated rims on the B faces and circumvallate papillae (usually sunk under the general level of the surrounding surface) on the A faces of both endothelial fronts. For convenience, these appearances will be referred to hereafter simply as

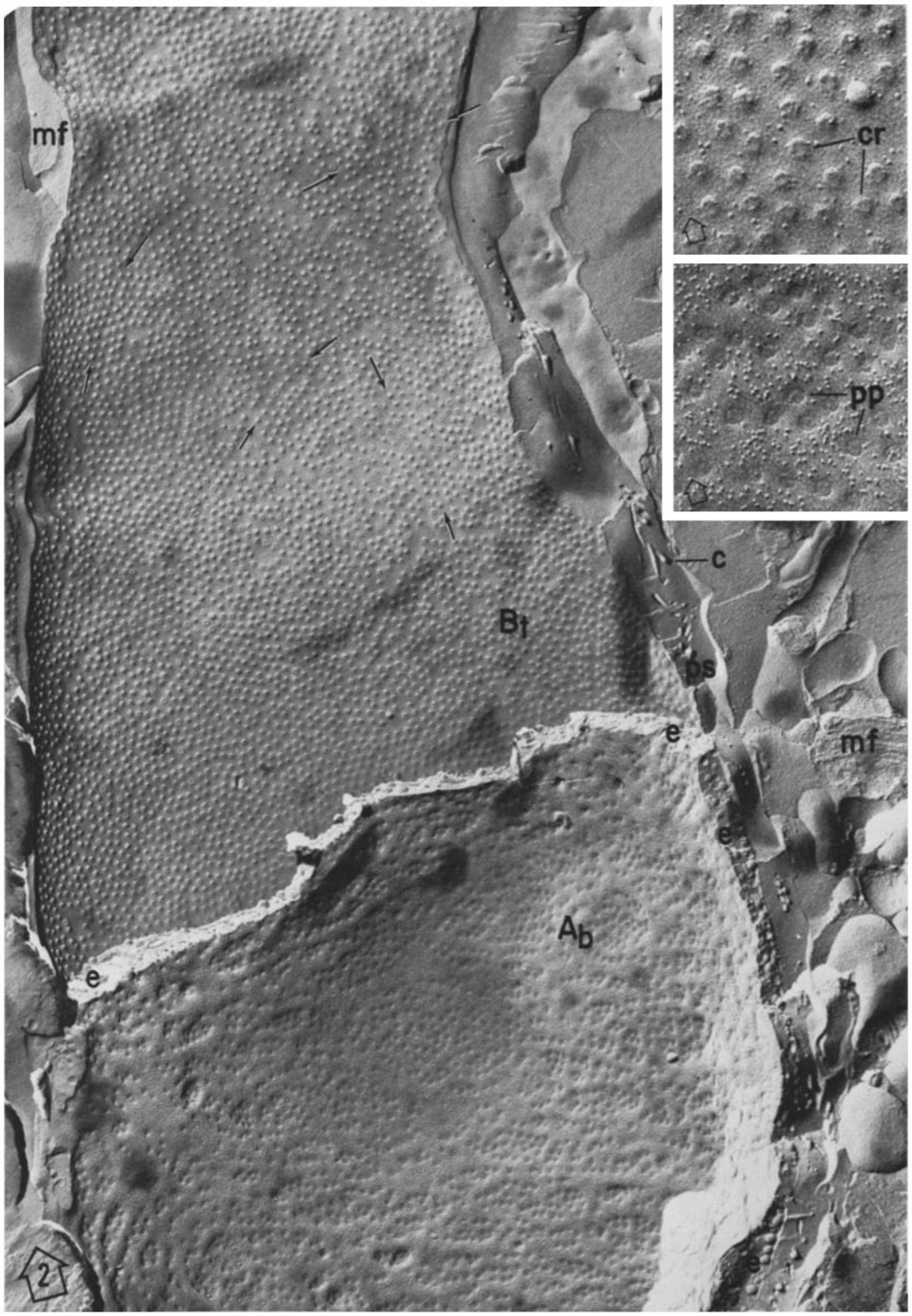

FIGURE 2 Myocardium capillary. The fracture followed the cleaved plane of the luminal membrane at A_b, broke through the endothelium at *e*, and then followed the cleavage plane of the plasmalemma on the tissue front at B_f. The circumvallate papillae which mark the broken necks of the plasmalemmal vesicles on the A_b face are shown at a higher magnification in the lower inset. The upper inset magnifies the complementary craters found on the B_f face. Note the difference in particle frequency between the two faces (best seen by comparing the insets), the tendency of the vesicle openings to form linear arrays (arrows), and the imperfect hexagonal lattice formed by the craters in the upper inset. × 17,000; insets: × 67,000.

craters or circumvallate papillae, respectively. In favorable specimens (cleaved membranes abutting against fractures across the endothelium), these structures, which measure 20–40 nm in diameter, can be reliably identified as fractures through vesicular stomata, usually through vesicular necks, since vesicles found deep in the endothelial cytoplasm are considerably larger (64–72 nm in diameter) (Figs. 4 and 5). The two appearances are complementary and represent different views of the same type of fracture, the ridge of the crater and the vallum of the papilla marking the beginning of the line of fracture of the outer membrane leaflet. The end of the fracture of the same leaflet is occasionally seen as a distinct line within the vallum of the circumvallate papillae.[2] The depth of the craters and the protrusion of the papillae are variable, which suggests that in some cases the openings are occupied by contained material, or that the fracture does not occur at the same level in all vesicles. The second alternative is supported by the occasional occurrence of apparently intact and sometimes distorted vesicles on the B faces (Figs. 16 and 17). In such cases, it appears that the vesicular neck has not been fractured and that the cleavage has peeled away the whole vesicle less half of its membrane. The complementary image appears, with the same low frequency, on A faces in the form of a deep depression (Figs. 9 and 15 b).

Besides clearly recognizable craters and papillae, both faces bear smaller (18–20 nm in diameter) structures which range in appearance from depressions to protruding rings or clusters of particles (Figs. 16 and 17). They may represent early phases in vesicle fusion to the plasmalemma or late phases in vesicle detachment. Alternatively, they may mark membrane sites specialized for vesicle fusion and fission.

FREQUENCY AND DISTRIBUTION: Figs. 2 and 3 demonstrate the strikingly high frequency of vesicle openings on each cell front and Table II gives quantitative data bearing on this point.[3] The frequency varies from ~30 to 130 vesicular stomata per μm^2 in the capillaries of the diaphragm and from ~40 to 145 vesicular stomata per μm^2 in those of the myocardium, the average values being slightly higher for the latter (89 openings per μm^2) than for the former (78 open-

[2] This rare detail appears more clearly in the circumvallate papillae and craters produced by fractures through fenestrae (see Figs. 11 a and 16) presumably because their diameters are larger.

[3] Table I gives 875 vesicles/μm^3, hence 218 vesicles in a volume of 1 × 1 × 0.25 μm, the average cell cytoplasm volume behind 1 μm^2 of endothelial surface. Table II gives 59 and 97 open vesicles per μm^2 of blood front and tissue front, respectively. The difference (62) represents the number of vesicles located in the interior of the cytoplasm, in the volume considered.

FIGURE 3 Blood capillary, diaphragm. The fracture reveals an A_f face, cuts through the endothelial cytoplasm at *e* (exposing numerous plasmalemmal vesicles), and uncovered the B_b face before breaking into the plasma (*pl*). A comparison with Fig. 2 indicates that the presence of craters and a low frequency of intramembranous particles characterize B faces irrespective of their location. The same applies for the occurrence of circumvallate papillae and a high frequency of intramembranous particles for the A faces. × 63,000.

FIGURE 4 Myocardium. Small sector of a cross fracture through the endothelium (*e*) of a blood capillary. Replicas of scooped (face A, short arrow) or protruding (face B, long arrow) vesicles appear on the blood front (v_1), interior of the cell (v_2), and on the tissue front (v_3). Note the chain of three vesicles (v_4) opening on the latter. The micrograph helps relating the opening of plasmalemmal vesicles with the circumvallate papillae (*pp*) seen on the A faces. × 103,000.

FIGURE 5 Pancreas, nearly transverse fracture through the endothelium, and a pericyte of a blood capillary. The fracture path moves from the plasma (*pl*) along the B_b face, through the endothelial cytoplasm (*e*) and along the A_f face. A number of vesicle openings are located astride the line of change in the direction of fracture from membrane to endothelial cytoplasm. Such instances make possible a reliable identification of openings with craters (*cr*) on the B face and with papillae (*pp*) on the *A* face. Note that the papillae can be seen only in conjunction with protruding vesicles and craters only when the vesicles have been scooped away. × 81,000.

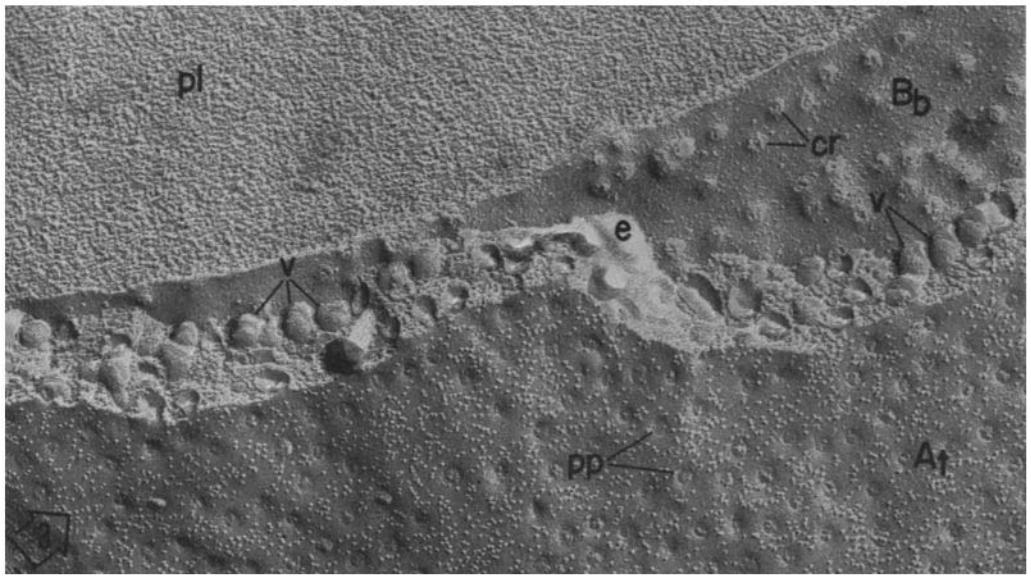
pl
Bb
cr
v
e
v
pp
At
3

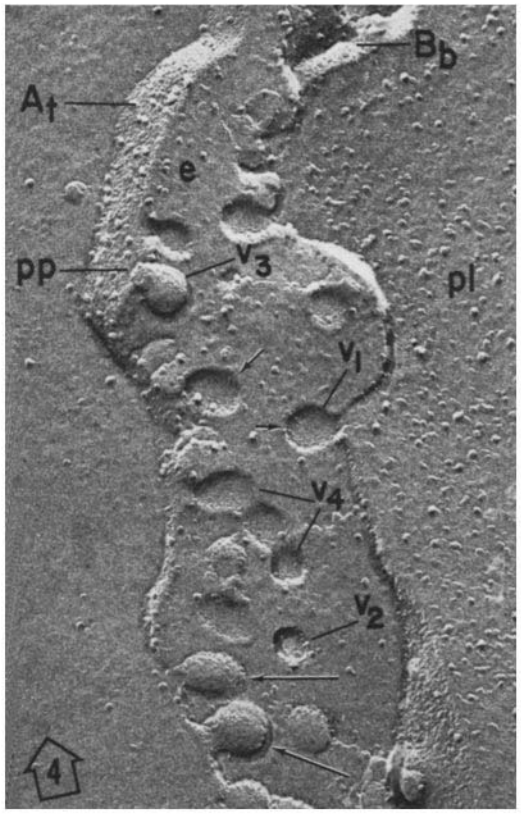
Bb
At
e
pp
v3
pl
v1
v4
v2
4

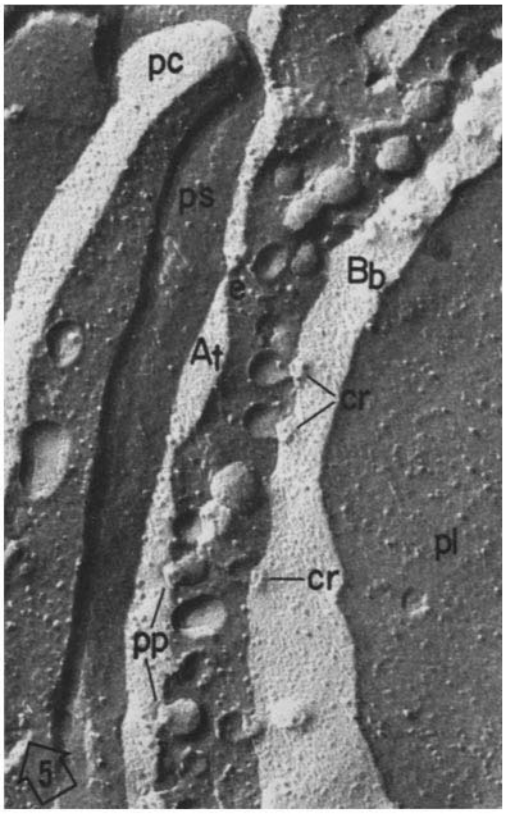
pc
ps
Bb
e
At
cr
pl
cr
pp
5

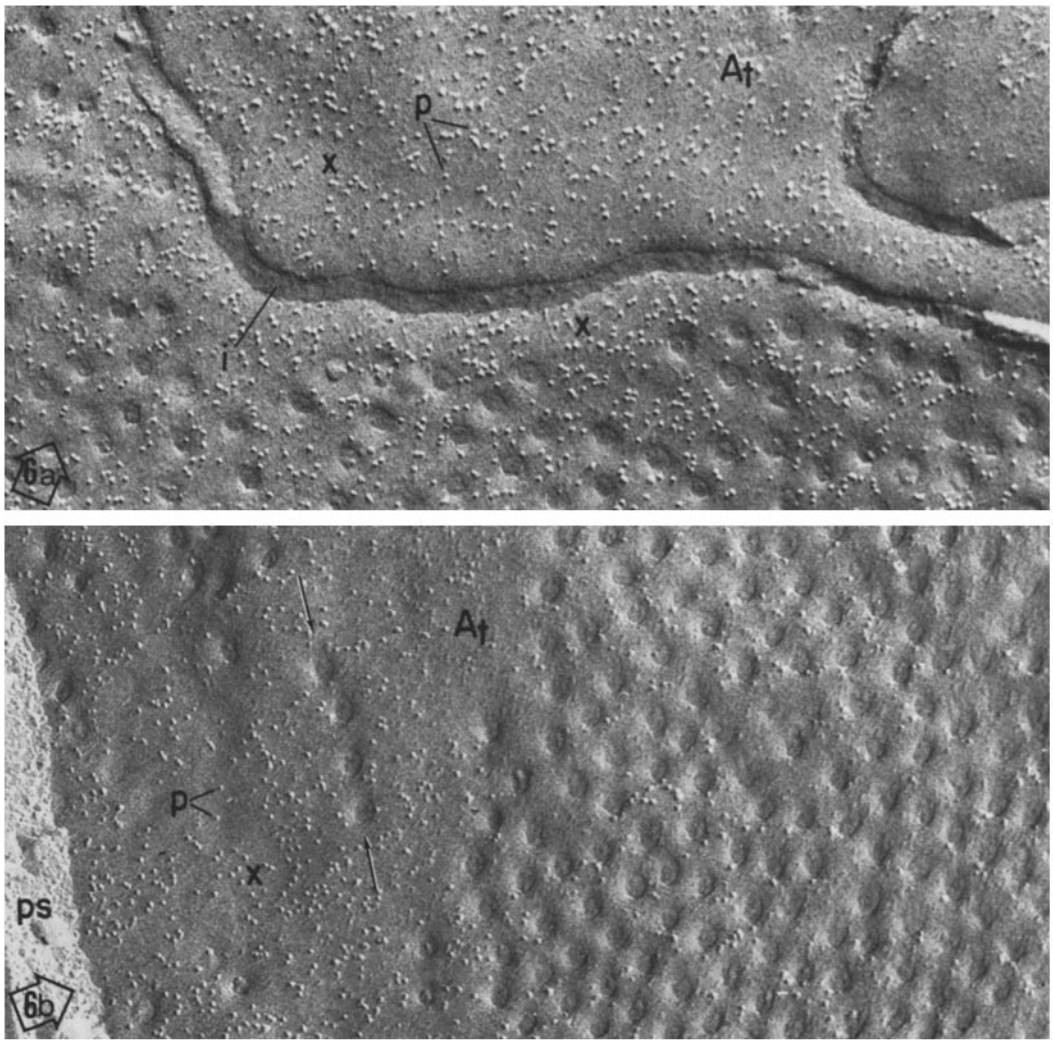

FIGURES 6 *a* and *b* Endothelium of a blood capillary in the diaphragm. A_t faces. Note: the abluminal, unusually large opening of an intercellular space at *i*, the high frequency of intramembranous particles over areas free of vesicle openings (*x*) and their absence (or very low frequency) over the openings themselves. Note also a linear array of vesicular openings (arrows), and the imperfect hexagonal lattice formed by vesicular stomata in the lower half of the field in Fig. 6 *b*. × 82,000.

ings per μm^2). In favorable specimens in which the nucleus can be located under a given area (Fig. 7), it appears that the local frequency of open vesicles is comparable to that shown in Table II. The frequency of vesicular stomata is considerably lower in visceral capillaries: $\sim 25/\mu m^2$ in the pancreas and $\sim 10/\mu m^2$ in the jejunal mucosa.

In the case of muscle capillaries, the density of vesicular openings appears to be higher (by 20–40%) on the tissue than on the blood front. The figures should be taken as maximal values which may be affected in part by the relatively small size of the blood front samples we had available for counting (¼ of the total area examined).

The fractional area occupied by vesicle openings on both endothelial fronts amounts to ~5% in the capillaries of the diaphragm, 7.3% in those of the myocardium, 2.5% in those of the pancreas, and 0.8% in those of the jejunal mucosa (Fig. 19).

In muscular capillaries, vesicular openings

TABLE II

Frequency of Vesicle Stomata and Fenestrae on Endothelial Surfaces

Type of capillary*	Aggregated area examined‡	No. of vesicular stomata‡ fenestrae counted	Vesicular stomata/μm^2		Fenestrae/μm^2 (range)
			Blood front (range)	Tissue front (range)	
	μm^2				
Muscular					
Diaphragm	87.8	7,848	59 (30–94)	97 (66–132)	
Myocardium	122.5	11,269	67 (39–98)	110 (64–144)	
Visceral					
Pancreas	80.5	3,071	32 (0–66)	21 (5–67)	15 (2–31)
Jejunal mucosa	91.8	3,399	11 (0–19)	9 (0–22)	26 (6–56)

* For each organ or tissue, replicas of 12–14 capillaries were examined.

‡ Covers the entire endothelial surface except the parajunctional zones.

have the tendency to cluster over large areas separated by regions of low density or alleys free of stomata. Within these clusters, they appear at 80 to 140 nm center to center distance from one another, often so closely grouped that there are few sites where additional vesicle openings can be fitted. Notwithstanding this impressive crowding, instances of close packing are extremely rare (Fig. 6 b). More often (Fig. 2), the openings are arranged in linear series at an average spacing of ~80 nm (center to center). This feature is particularly evident in vessels larger than capillaries in which the frequency of vesicles is generally lower (Fig. 8 c).

In visceral capillaries the distribution of vesicular openings is affected by the presence of clustered fenestrae, and for this reason it will be described later on in connection with the latter.

Fenestrae

STRUCTURAL ASPECTS: In visceral capillaries, the cleaved membranes of endothelial surfaces reveal a second type of rounded openings with diameters ranging from 50 to 80 nm (Fig. 13). By their continuity with both endothelial fronts, as seen especially on cross fractures, they can be reliably identified as endothelial fenestrae (Figs. 11 and 12).

Except for their larger diameter, the general appearance of the fenestrae is similar to that found for vesicle openings. They appear as circumvallate papillae on A faces and craters on B faces (Figs. 11 a and b). The transition from one appearance to the other can be easily seen on different sectors of practically every fenestra located astride a line of fracture through the endothelium (Figs. 11 and 12). In many cases the fenestrae are partially or completely filled by a plug which is usually free of or covered by only a few associated particles (Fig. 11 b). The plug may correspond to a fenestral diaphragm, but the identification is uncertain.

FREQUENCY AND DISTRIBUTION: The density of the fenestral population (Table II) is almost twice (1.7×) higher in jejunal (26 fenestrae per μm^2) than in pancreatic capillaries (15 fenestrae per μm^2), their aggregated areas accounting for 9.5 and 6%, respectively, of the total endothelial surface (Fig. 19). The data in Fig. 19 and Table II suggest that the frequency of vesicles decreases as that of fenestrae increases from one type of visceral capillary to another.

The fenestrae are distributed in clusters, which are large and irregular in jejunal capillaries (Figs. 8 a and 9) and small but more clearly outlined in those of the pancreas (Fig. 10). In general there is little intermixing of fenestrae and vesicular openings except at the periphery of the clusters. Within the latter, the fenestrae occasionally appear distributed like the vesicular stomata in linear series at an average spacing of 130 nm center to center. (Figs. 8 a and b and 17).

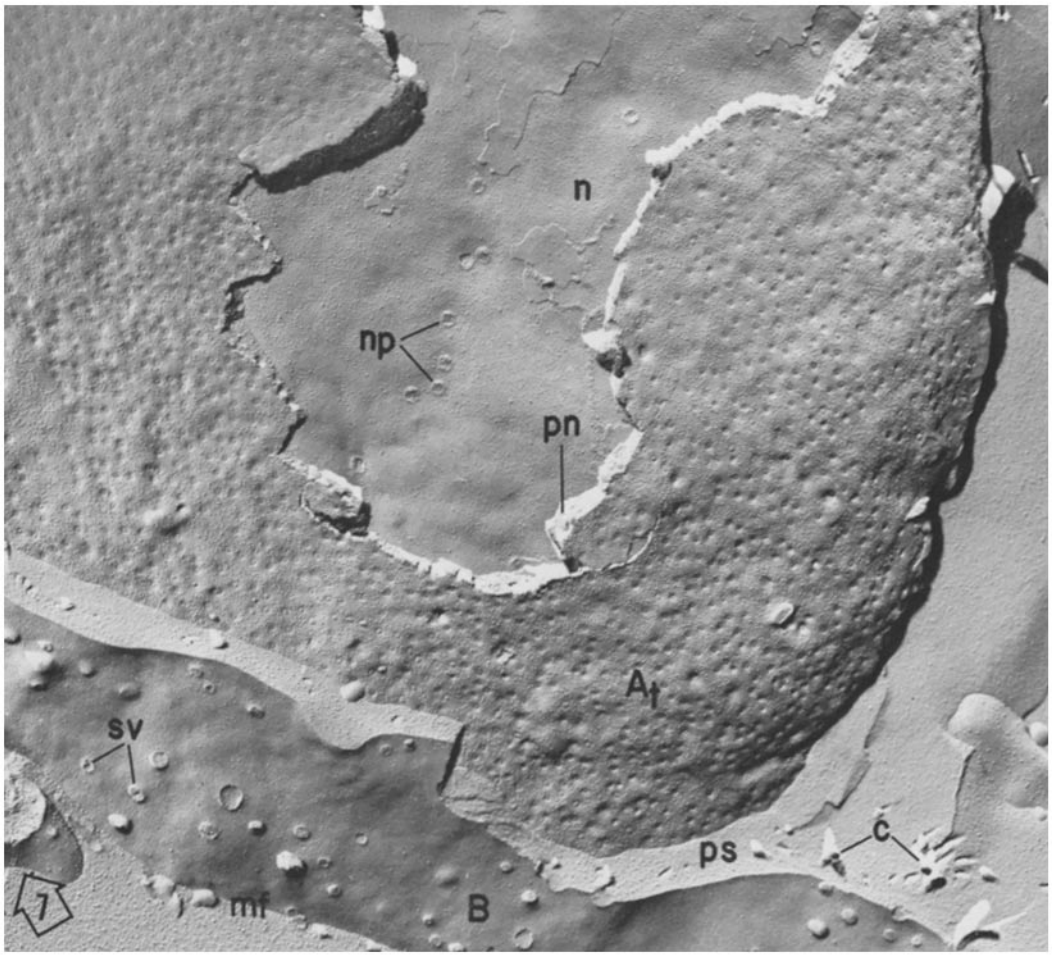

FIGURE 7 Myocardium. The fracture plane reveals the B face of the plasmalemma of a muscle fiber at B, breaks through a pericapillary space (*ps*) and exposes thereafter the A_f face of an endothelial cell at the level of the nuclear region. The two membranes of the nuclear envelope and a few nuclear pores (*np*) are seen through a "window" in the perinuclear cytoplasm (*pn*). Note the high frequency of vesicle openings in the nuclear region. × 20,000.

Parajunctional Zone

The bands of endothelial surfaces free of vesicular stomata and fenestrae which are found along the intercellular boundaries have an average width of 0.5 μm for each neighboring cell. For the two adjoining cells this gives a ribbon-like parajunctional area with a mean width of 0.7–1 μm on both endothelial fronts and in all four types of capillaries studied (Table III, Figs. 8 a, 14, and 15 a and b). Each area appears to form a quasi complete zone, since on 75–90% of the boundaries' length the band is symmetric, i.e., it involves both cells; on the rest it is asymmetric, i.e., it is restricted to one cell only.

Intercellular Spaces

The length of the intercellular spaces is 3.2 and 1.4 μm/μm length of muscular and visceral capillaries, respectively (Table IV). This value reflects a relatively modest extent of meandering since the increase over smoothed out distances along the perimeter of the cells is of ~50% only. For all capillaries studied, the width of the intercellular spaces varies from 16 to 28 nm on the

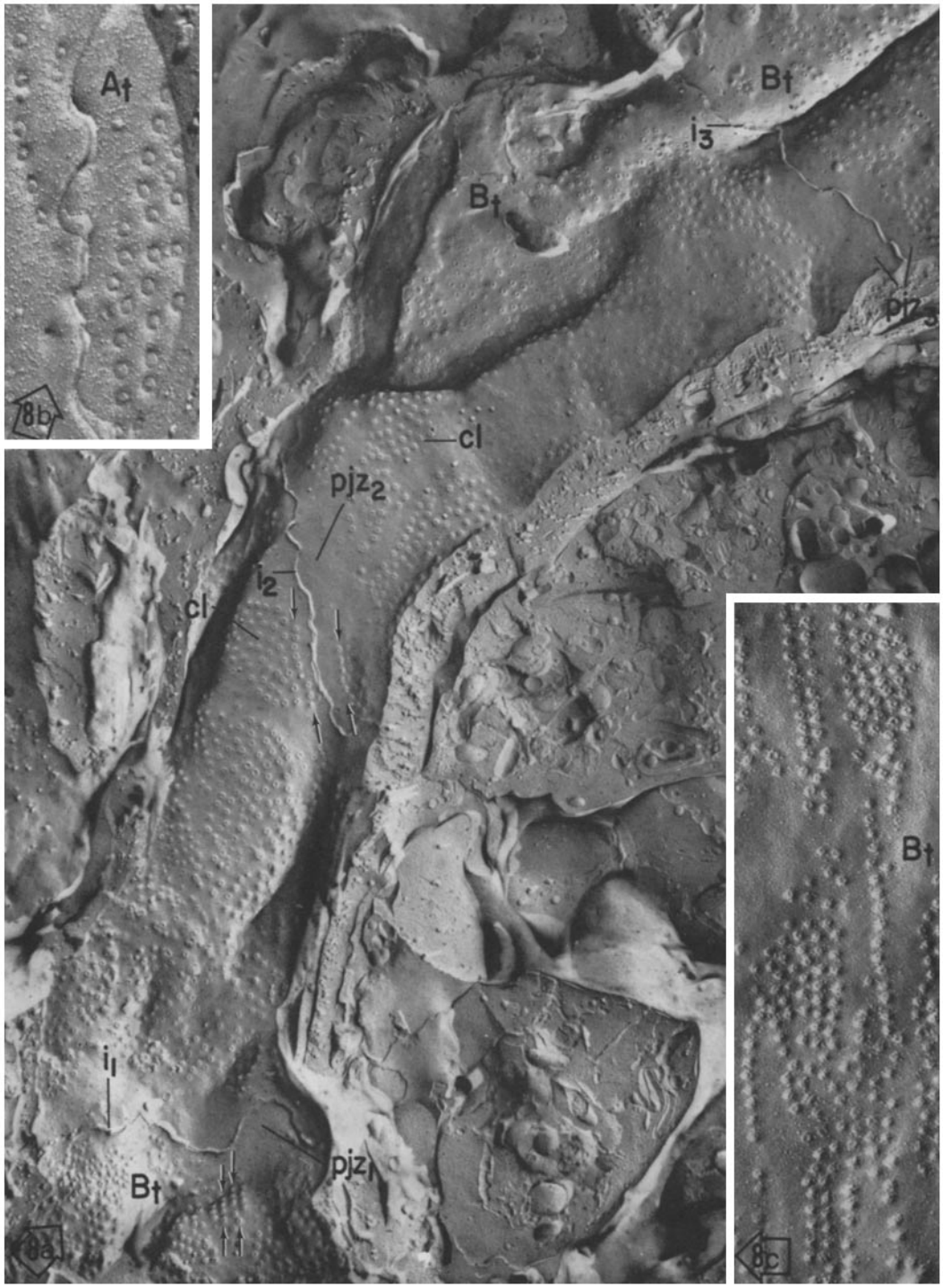

FIGURE 8 *a* Jejunal villus. B_t face of the fenestrated endothelium of a capillary exposed over an unusually long distance (~25 μm). The cleavage reveals the full length of two endothelial cells and partly that of two others. The intercellular lines run transversely to the long axis of the vessel at i_1 and i_3 and obliquely to it at i_2. Parajunctional zones ($pjz_{1,2,3}$) (free of vesicular and fenestral openings) are seen along each of the intercellular lines. The fenestral openings occur in clusters (*cl*) separated by smooth alleys. Within the clusters, the fenestrae have the tendency of occurring in linear arrays (arrows). This tendency is convincingly illustrated by the occurrence of isolated rows of fenestrae as in Fig. 8 *b* (A_t face, jejunal villous capillary). Vesicle openings have the same tendency especially in larger vessels as shown in Fig. 8 *c* (B_t face of the endothelium of a relatively large vessel in the diaphragm). Fig. 8 *a*: × 10,000; Figs. 8 *b* and *c*: × 32,000.

FIGURE 9 Jejunal capillary. An A_t face is exposed over a large area. The corresponding B_b face appears through a fracture of the endothelium at B_b. The micrograph illustrates the large, poorly outlined clusters of fenestrae in this type of capillary. The deep depressions marked by arrows mark the site of vesicles peeled away with the outer membrane leaflet at the time of cleavage. × 16,000.

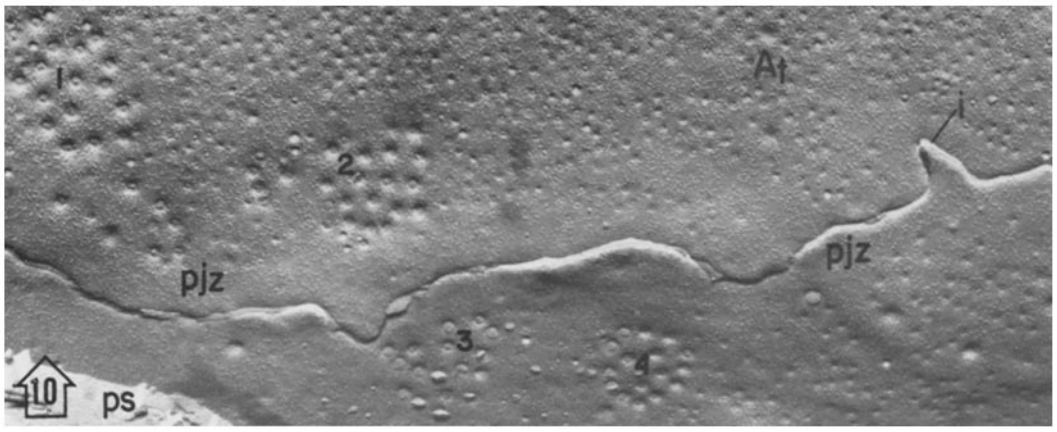

FIGURE 10 Pancreas capillary. A_t face crossed lengthwise by an intercellular line (*i*). Four (one to four) small well-defined clusters of fenestrae are shown in this field, they are surrounded by numerous unevenly distributed vesicular openings, or are bordering on the parajunctional zone (*pjz*). × 19,000.

tissue front, and from 10 to 21 nm (14 nm average) on the blood front of the endothelium. These values are not corrected for included half-membranes.

The examination of a relatively large number of transverse sections of blood capillaries indicates that most muscle capillaries have two intercellular junctions, while their visceral counterparts have only one, which means that the endothelial tunic is made up of two cells in muscular capillaries and one cell only in visceral capillaries at most points along the vessels' long axis. In agreement with these findings is the impression that most intercellular lines (~80%) are oriented parallel to the long axis of the vessel in muscular capillaries, and transverse to the same axis (~60%) in visceral capillaries.

Endothelial Cell Dimensions

Due to the relatively limited number of specimens in which the cleavage plane goes from cell boundary to cell boundary (see Fig. 8), we have collected only few data on the length of endothelial cells in the different types of capillaries examined. The values so far obtained vary from ~20 μm to ~10 μm for diaphragm and jejunum capillaries, respectively (Table V). This is in contrast with the width and the thickness of the endothelial cells which have been reliably determined on large samples of properly oriented sectioned or freeze-fractured specimens (Table V). Since data on the third dimension (length) are much more limited and hence less reliable, we have normalized our data to unit length (1 μm) of the blood front of the capillary wall (Table VI).

Pericytes

Pericytes are easily recognized in replicas of all capillary vessels on account of their multifold pseudopodia (Fig. 18) which embrace, and appear partially sunk into, the endothelium. The cleavage surfaces of their membranes are marked by vesicular stomata, but the frequency of the latter is considerably lower than in endothelial cells (Fig. 18).

DISCUSSION

Table VII compares our data with those already available in the literature on muscle capillaries. The higher frequency of plasmalemmal vesicles per μm^3 recorded by Casley-Smith (13) and Wolff (11) are probably due to species differences or differences in sampling. The much lower frequency of vesicle openings per unit area reported by Leak (19) in heart capillaries may result from the inclusion of larger vessels in his samples (see Figs. 2 and 3 in reference 19).

Table VIII allows a similar comparison for the fenestrae of visceral capillaries. Measured fenestral diameters are larger in freeze-cleaved specimens than in sectioned material; the difference could be explained, at least in part, by difficulties encountered in measuring the ~600 Å

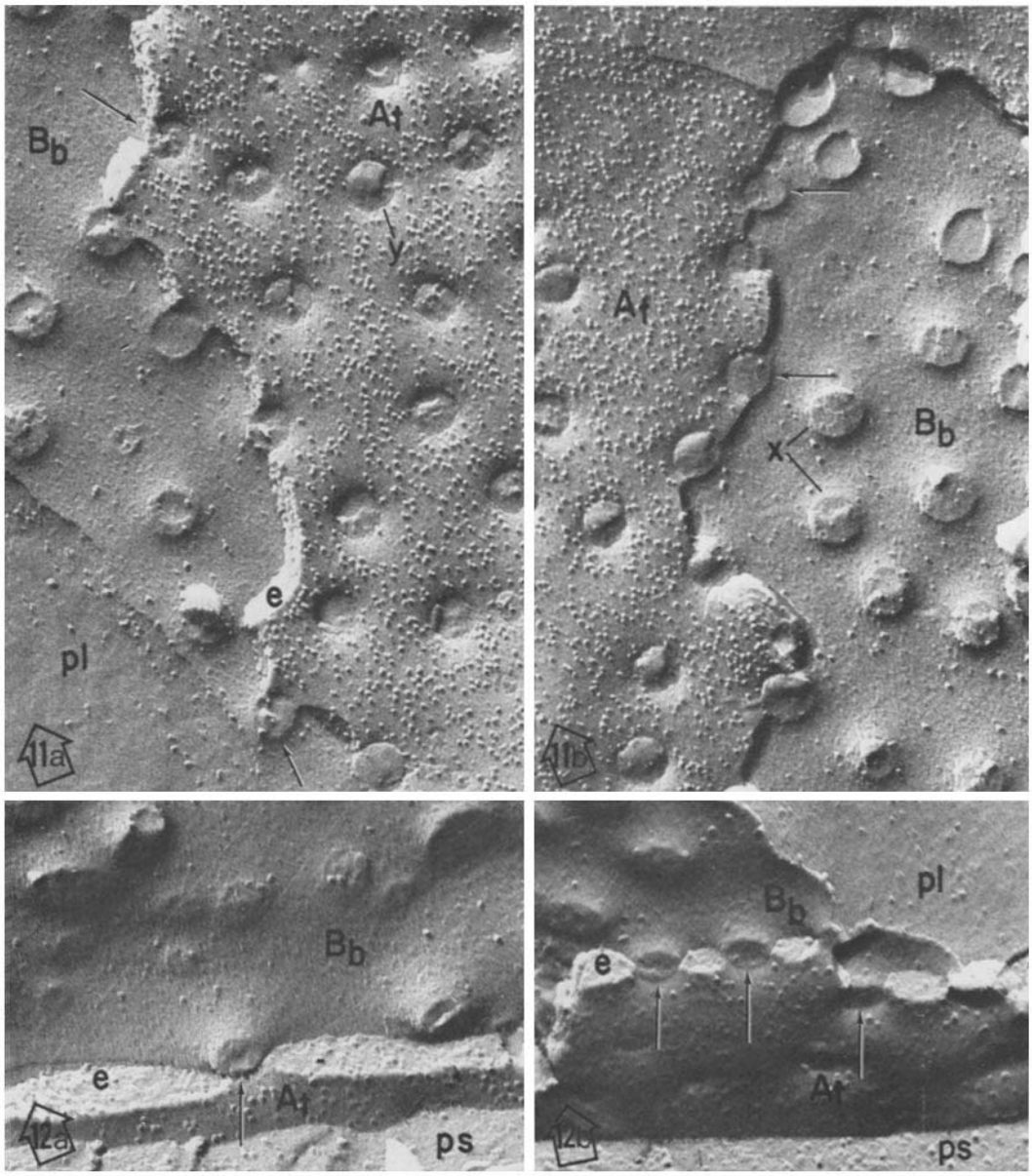

FIGURES 11 *a* and *b* Pancreas capillary. In both figures the fracture reveals both B_b and A_t faces and cuts through the endothelium (*e*) along a series of fenestrae. This situation allows the reliable identification of the fenestrae with craters on the B faces and circumvallate papillae on the A faces. In the papilla marked *y*, a fine inner arc (seen from 3 to 6 o'clock) marks the line of fracture of outer membrane leaflet. Note the change in appearance from crater to papilla for the fenestrae located along the fracture line through the endothelium (arrows). Note also the considerable variation in the protrusion and surface detail of the papillae as well as in the depth of the craters. Some of the latter have a flat or irregular top (*x*) (instead of a scooped one). × 82,000.

FIGURES 12 *a* and *b* Pancreas capillary. The micrographs reveal B_b and A_t faces separated by fractures through the endothelial cytoplasm (*e*). Along the fracture line the transition from craters (on the B_b face) to papillae (on the A_t face) is clearly visible for a number of fenestrae (arrows) which appear in slightly oblique view. × 96,000.

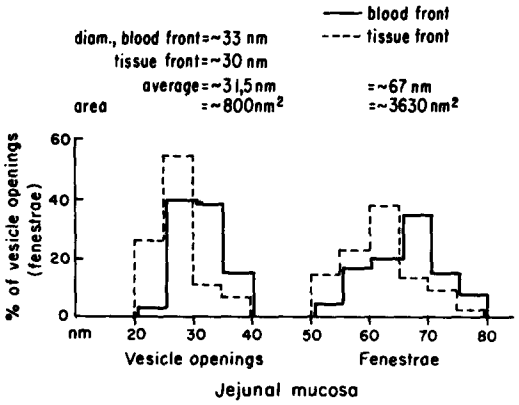

FIGURE 13 Size distribution of vesicle openings and fenestrae on both endothelial fronts in a visceral capillary (jejunal mucosa). Numbers counted: 138 fenestrae, 114 vesicles.

diameter of a normally sectioned fenestra, in sections the thickness of which approaches the same value. Fenestral frequency appears to be higher and fenestral fractional area larger in renal peritubular capillaries (15, 23, 24) than in the capillaries of the pancreas and of the jejunal mucosa we have examined. The extensive fenestration of the peritubular vessels is probably related to their high permeability to proteins recently investigated by Venkatachalam and Karnovsky (25).

Our morphometric data provide quantitative information collected on relatively large samples and bear on a number of structural features of current functional interest. Some of the data, e.g., capillary diameters and thickness of the endothelial layer, concern aspects already covered by light microscopy (26–29) and less extensively by electron microscopy (1–3, 30–32). The rest refers to fine structural features (plasmalemmal vesicles, fenestrae, intercellular spaces) whose role in capillary permeability is still under investigation. Data concerning the dimensions and frequency of fenestrae and the fractional area for which they account should be immediately useful in the current discussions on structural aspects of capillary permeability, since the diameter of these structures approaches closely that postulated for the large pores, (cf. 33, 34) and since there is evidence that the fenestrae are permeable to molecules large enough to act as large pore probes (7, 8). As already discussed in a previous paper (8), their fractional area is, however, much larger than that postulated for

TABLE III

Relative Area and Distribution of Parajunctional Zones in Capillary Endothelium

Type of capillary*	Average area/ intercellular line length (range)‡	Distribution§	
		Symmetric	Asymmetric
	$\mu m^2/\mu m$	%‖	%‖
Muscular			
Diaphragm	0.75 (0.3–2.1)	66 (41–89)	34 (11–59)
Myocardium	0.96 (0.3–2.1)	73 (55–91)	27 (9–45)
Visceral			
Pancreas	0.80 (0.4–1.6)	78 (47–89)	22 (11–53)
Jejunal mucosa	0.88 (0.3–2.0)	91 (66–98)	9 (2–34)

* For each vascular bed, the sample examined included 6–10 capillary replicas, 80–110 μm length of intercellular lines, and ~70 to 95 μm^2 of parajunctional zones.
‡ Differences between the two fronts of the endothelium ranged from 0.1 (pancreas) to 0.35 (myocardium).
§ Differences between the two fronts of the endothelium ranged from ~5 to 25%.
‖ Percentage of the intercellular line length.

TABLE IV

Fractional Area Occupied by Intercellular Spaces on the Blood Front of Capillary Endothelium

Type of capillary*	Intercellular spaces			
	Mean number	Average length‡	Area§	% of blood front area
		μm	μm^2	
Muscular				
Diaphragm, Myocardium‖	2	3.2	0.04	0.2
Visceral				
Pancreas, Jejunal mucosa‖	1	1.4	0.02	0.08

* Measurements made on 6–10 capillary replicas for each vascular bed.
‡ Calculated per micrometer length of capillary.
§ Calculated by using 14 nm average width of the intercellular spaces in all types of capillaries.
‖ For capillary dimensions, see Table V.

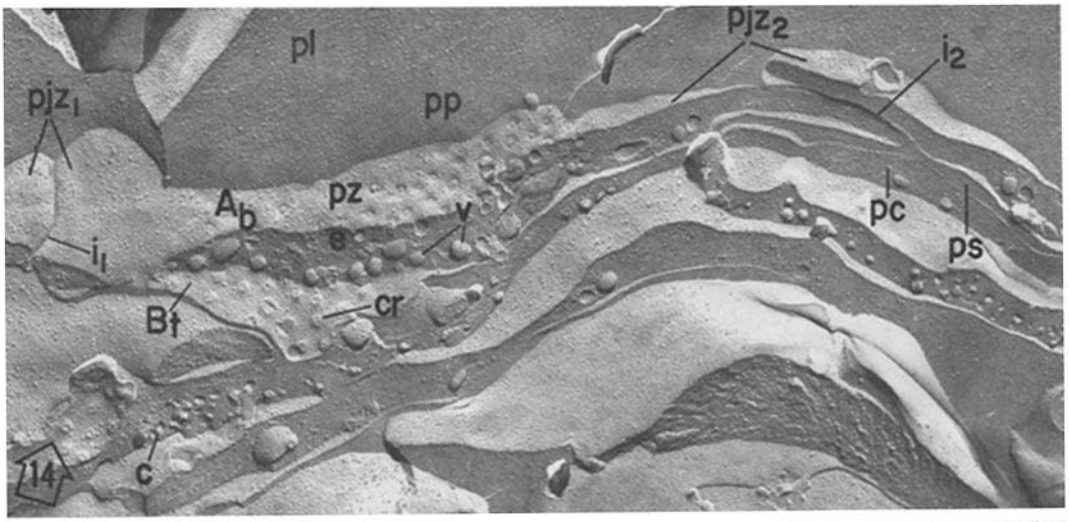
pl
pjz2
i2
pjz1
pp
pz
Ab
v
e
pc
ps
i1
Bf
cr
c
14

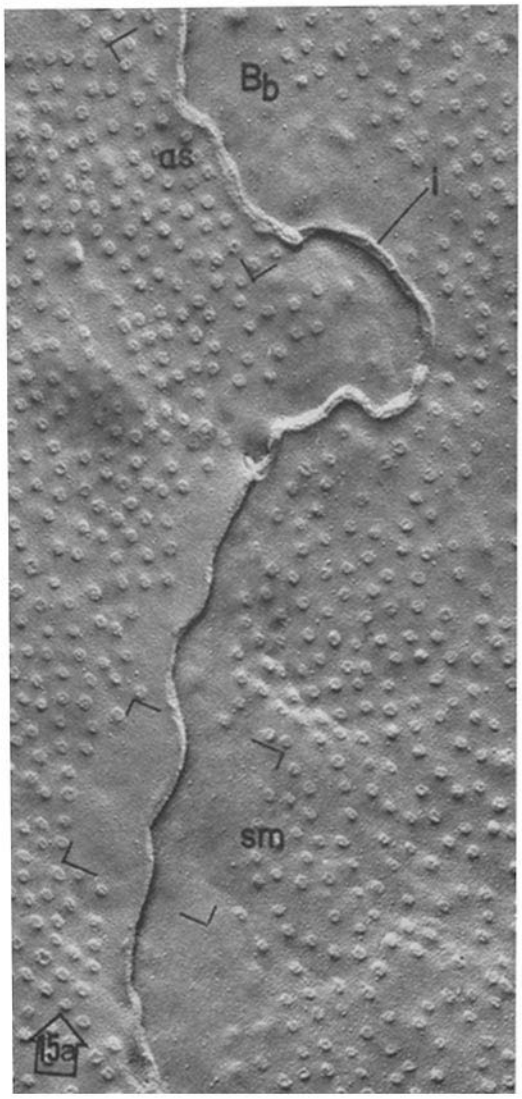
Bb
as
l
sm
15a

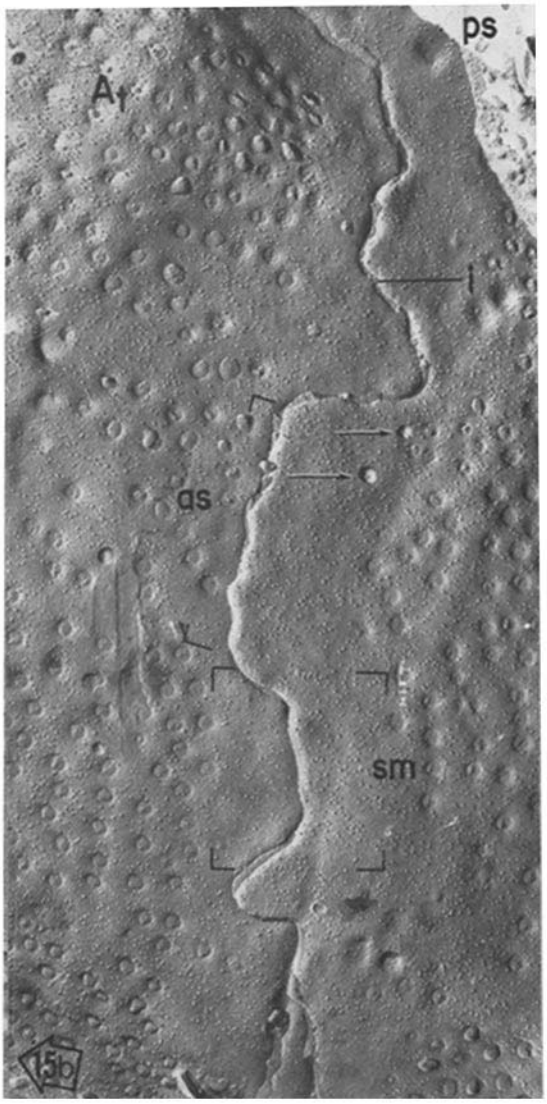
ps
Af
l
as
sm
15b

TABLE V

Average Diameter of Different Types of Capillaries and Average Dimensions of Endothelial Cells

Type of capillary	Average inner diameter*	Endothelial cell		
		Width‡	Length§	Peripheral zone thickness*
	μm	μm	μm	μm
Muscular				
Diaphragm	5 ± 1	8.3 ± 1.2	22 ± 2.3	0.25 ± 0.1
Myocardium	6.6 ± 1	9.2 ± 1.4	17 ± 2.0	0.25 ± 0.1
Visceral				
Pancreas	7.2 ± 1.7	11.4 ± 1.3	18 ± 2.1	0.30 ± 0.15
Jejunal mucosa	8 ± 2.1	19.2 ± 2.1	10 ± 3.4	0.16 ± 0.1

* For each vascular bed, measurements were made on an average of 80 capillary profiles on both sectioned or cross-fractured specimens.

‡ Width measurements were made only at the level of the nuclear or organelle region.

§ Determined on ~5 replicas of freeze-cleaved specimens for each type of capillary.

TABLE VI

Frequency and Aggregate Area of Vesicular Stomata and Fenestrae per 1 μm Capillary Length on the Blood Front of the Endothelium

Type of capillary*	Total area	Blood front			
		Vesicular stomata		Fenestrae	
		No.	Area‡	No.	Area‡
	μm²		μm²		μm²
Muscular					
Diaphragm	15.7	926	0.75		
Myocardium	20.7	1,387	1.11		
Visceral					
Pancreas	22.6	723	0.57	339	1.18
Jejunal mucosa	25.1	276	0.22	653	2.26

* See Table V for capillary dimensions and Table II for vesicle stomata frequency per μm^2.

‡ Average unit areas used: vesicular stoma = 800 nm^2, fenestra = 3500 nm^2.

the large pore system. The discrepancy can be explained by the existence of diaphragms reducing the effective diameter of the fenestrae, and, in the opposite direction, by the involvement of plasmalemmal vesicles in the transport of large molecules. It follows that in visceral capillaries not all the fenestrae function as large pores at all times, but it appears quite clearly that they are the best candidate for structural equivalents of the large pore system, the plasmalemmal vesicles assuming only a secondary role.

The intercellular spaces are open at their luminal end to gaps of ~14 nm and account for ~0.08 to 0.2% of the inner endothelial surfaces (or less if the figures are corrected for included half membranes). The last figure comes close to the early estimates of the aggregate area of the small pores (33). As already discussed in the literature, these spaces are either apparently closed or open to considerably smaller gaps at some distance from the lumen (1, 35, 36). Such

FIGURE 14 Jejunal capillary. Nearly transverse fracture of the capillary wall at the level of the peripheral zone (*pz*) and the parajunctional zones (*pjz*) of three endothelial cells. The fracture plane exposes A_b and B_t faces separated by a transverse break through the endothelial cytoplasm (*e*). The vesicle-free parajunctional zones pjz_1 and pjz_2 border on the intercellular lines i_1 and i_2. Between these two lines appears the peripheral zone (*pz*) of the middle endothelial cell with papillae (*pp*) on the A_b face, vesicles (*v*) in the interior of the cell, and craters (*cr*) on the B_t face. × 28,000.

FIGURES 15 *a* and *b* Partial views of parajunctional zones on the B_b face of a myocardium capillary (a) and on the A_t face of a jejunal capillary (b). In both cases, note the occurrence and distribution of symmetric (*sm*) and asymmetric regions (*as*). The deep depression marked by arrows in Fig. 15 *b* are "holes" left behind by vesicles peeled away with the outer membrane leaflet at the time of cleavage. Figs *a*: × 32,000; Figs *b*: × 28,000.

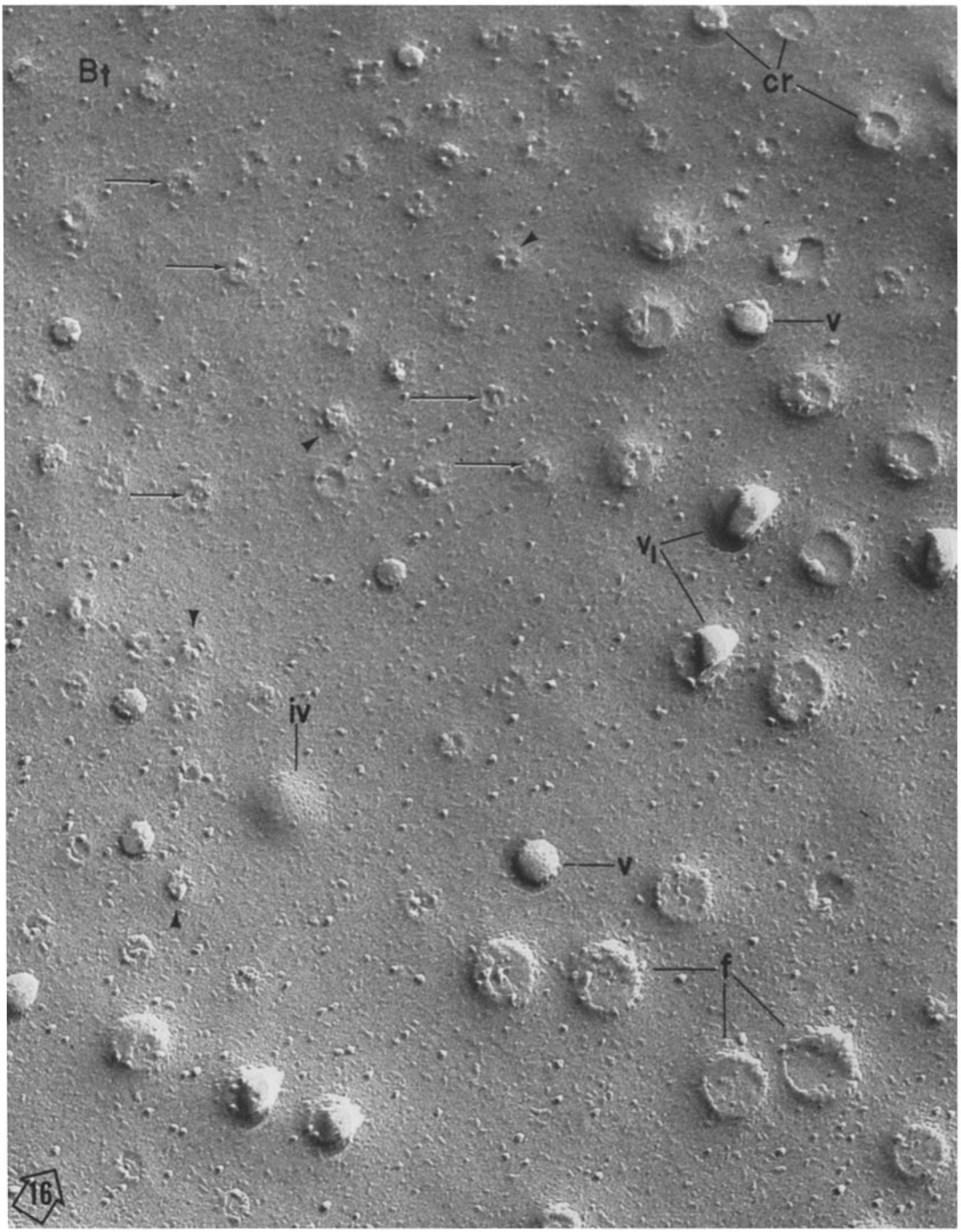

FIGURE 16 Pancreas capillary. In addition to the usual craters marking vesicular openings (*cr*) and fenestrae (*f*), this B_t face shows a few peeled vesicles (*v*), some of them torn aside (v_1), and a number of smaller structures which have the appearance of slightly protruding rings or small clusters of particles (arrows). Some of these structures are distributed in linear arrays (arrowheads). Note the fine arc of shadow within some of the craters in the lower right corner of the field: it marks the fracture line of the outer leaflet of the plasmalemma. The appearance of *iv* is assumed to represent the beginning of an invagination of the plasmalemma. × 101,000.

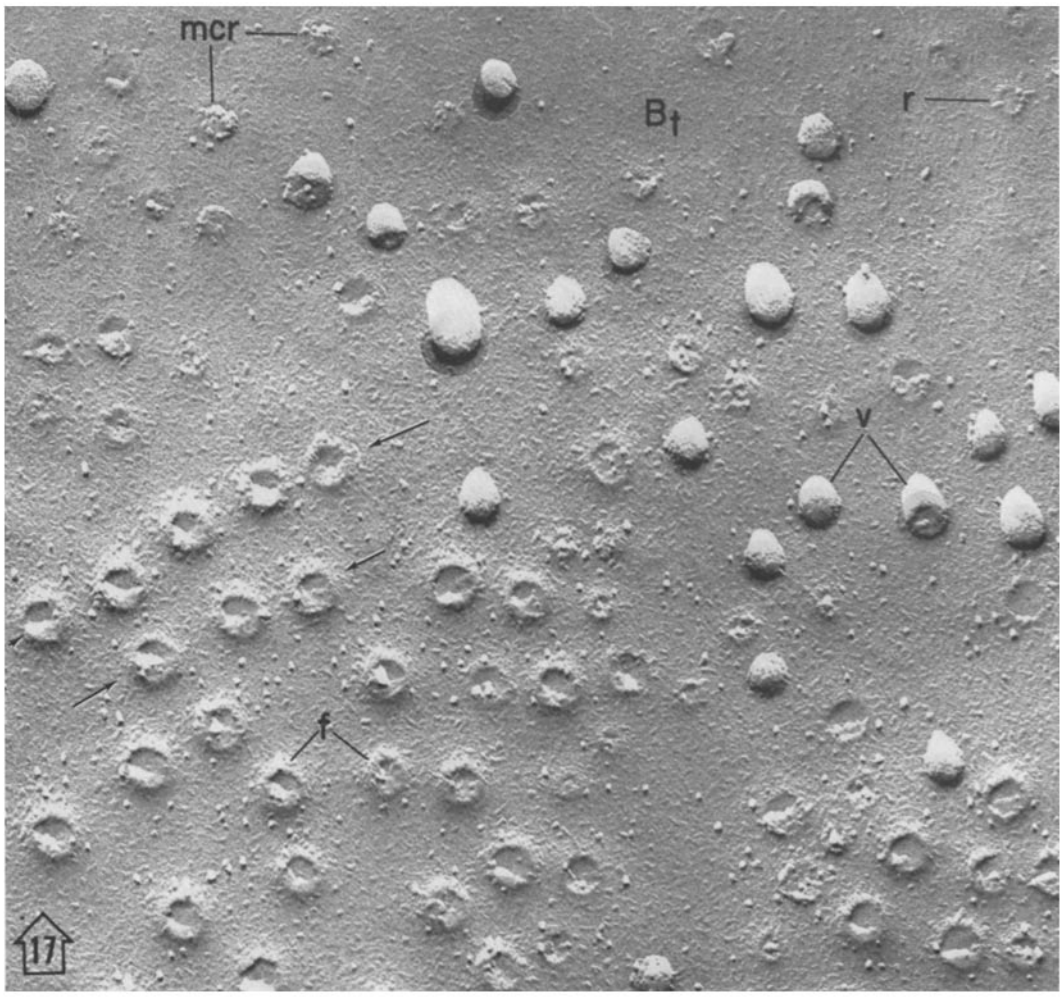

FIGURE 17 Jejunal villous capillary. This B_f face shows craters marking fenestrae (*f*), some of them disposed in linear arrays (arrows), whole vesicles (*v*) peeled away by the cleavage, miniature craters (*mcr*), and ring-line structure (*r*). As in Fig. 16 the latter (*mcr* and *r*) may represent specialized sites for vesicle fusion, initial phases in the fusion process, or late phases in vesicle detachment from the plasmalemma. × 80,000.

constrictions reduce drastically the aggregate area of the intercellular gaps, but since the path length across the endothelium is also drastically reduced, it is still possible that slits along the intercellular junctions represent the small pore system (cf. 37). Since reliable morphometric data on this point cannot be obtained at present, molecular probes appear to be a more suitable approach than morphometry for the localization of the small pore system.

The most impressive data concern the high frequency of plasmalemmal vesicles in muscle capillaries, the large fraction of endothelial volume for which they account, and the large amount of membrane they contribute to the cell (~40× the volume of the plasmalemma). The capacity of the vesicular system, i.e., the aggregate volume of the vesicular content, amounts to ~7% of the endothelial volume. All these data should be useful in assessing the role of the plasmalemmal vesicles in relation to different aspects of capillary permeability. The very high frequency of open vesicles on both fronts, particularly on the tissue front of muscular capillaries, is surprising es-

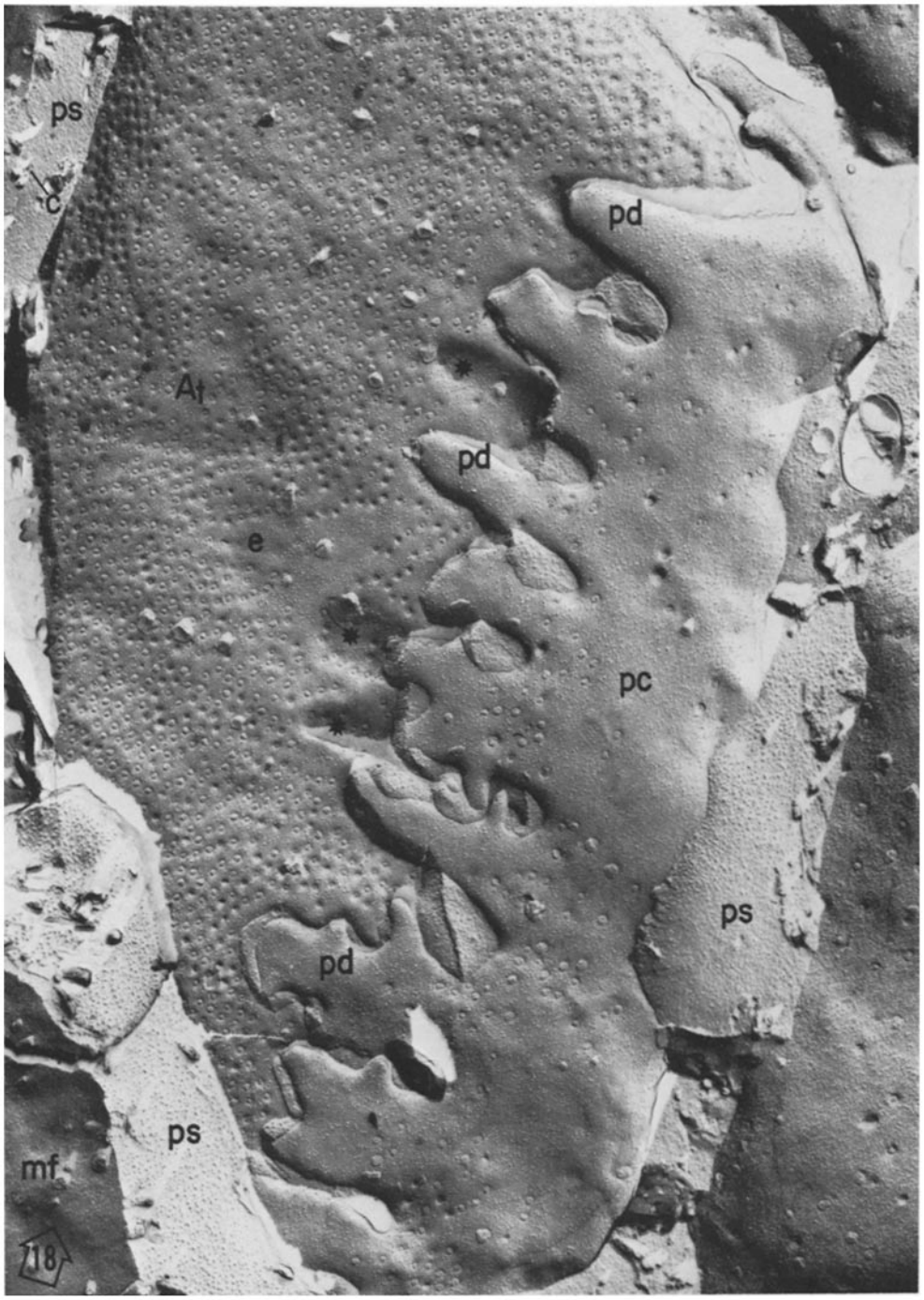

FIGURE 18 Diaphragm capillary. A_f face partially covered by a pericyte (*pc*) and the latter's numerous pseudopods (*pd*). The asterisks mark depressions left on the endothelium by pericyte pseudopods partially removed by the fracture. Note the striking difference in the frequency of vesicular openings between the endothelial cell (*e*) and the pericyte (*pc*). × 24,000.

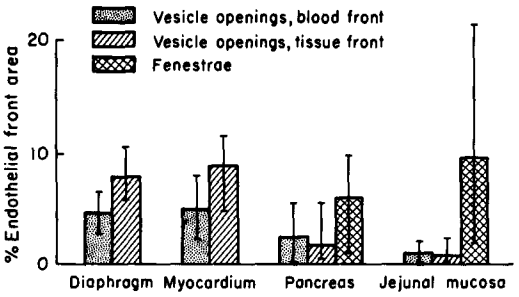

FIGURE 19 Fractional areas occupied by vesicle openings and fenestrae on the two endothelial fronts in the four types of capillaries studied. (Graph based on data presented in Table VI.)

pecially because within certain clusters of open vesicles there is hardly a place left for additional vesicles to open. The finding suggests that the open phase of the vesicles is relatively long, perhaps longer than assumed in the past (4, 38–40) and that incoming vesicles may fuse with already open vesicles instead of fusing directly with the plasma membrane on the corresponding cell front. Using the data in Tables I and II, it can be calculated that $\sim\frac{1}{3}$ of the total vesicle population is located in the interior of the endothelial cytoplasm, irrespective of the relationship of the corresponding vesicles, i.e., isolated or open to one front or the other via another vesicle.

In addition to appearances which can be reliably identified as vesicular openings or fenestrae, we have found on the cleaved surfaces of the endothelial plasmalemma particle clusters which occasionally take the forms of rings. Although more randomly distributed, such clusters are reminiscent of the sites described by Satir et al. (42, 43) in the plasmalemma of *Tetrahymena* and identified by them as fusion sites for micro-

TABLE VII

Vesicle Frequency in Capillary Endothelium (Comparative Data)

Tissue or organ	Animal	No. vesicles per μm^2				No. vesicles/μm^3	Observations	Refs.*
		Mean	Blood front	Inside	Tissue front			
Diaphragm	Rat					883 (421–2000)	Endothelium thickness = 0.2 μm	(1)s
						617 (406–1000)	Endothelium thickness = 0.4 μm	(1)s
	Mouse		125–135	175–300	125–135	1372	841 free + 531 attached/μm^3	(13)s
	Rat		59 (30–94)		97 (66–132)	684		(*S*)s,f
Skeletal muscle	Rat	15–200				200–2250		(11)s
Heart	Rat	120	106 (102–108)	73	117 (114–123)		Less numerous in perikaryon	(1)s
	Mouse	38	39		40, A faces 37, B faces		36/μm^2 in perikaryon	(18)f
	Rat		67 (39–98)		110 (64–144)	766		(*S*)f,s
Lung	Rat	37						(47)f
Pancreas	Rat		32 (0–66)		21 (5–67)	154		(*S*)f,m
Jejunal mucosa	Rat		11 (0–19)		9 (0–22)	118		(*S*)f,m

* s = sectioned specimens; f = freeze-fractured specimens; (*S*) = data in present paper.

TABLE VIII

Dimensions, Frequency and Fractional Area of Fenestrae in Capillary Endothelium (Comparative Data)

Tissue or organ	Animal	Fenestrae			Observations	Refs.*
		Diameter	Frequency/μm^2	Fractional area		
		nm		%‡		
Jejunum	Mouse	35–45		~10		(2)s
	Mouse				12 more numerous on venous ends	(5, 6)s
	Rat	67	26 (6–56)	9.5 (2.2–20.3)		(*S*)f
Pancreas	Rat	66	15 (2–31)	6 (0.7–11)		(*S*)f
Kidney§	Mouse	70	30	35		(23)s
	Rat	50			With diaphragm	(10)s
		65		14–25	Without diaphragm	
	Mouse	65	60	15		(15)f
	Rat	685 (52–100)			A faces	(24)f
		648 (60–68)			B faces	

= Comparable dimensions have been mentioned for the fenestrae of the capillary endothelium in the thyroid, adrenal cortex, ovary, testicle, and vagina (10).

* s = sectioned specimens; f = freeze-fractured specimens; (*S*) = data presented in this paper.

‡ Percentage of endothelial surface

§ Peritubular capillaries only.

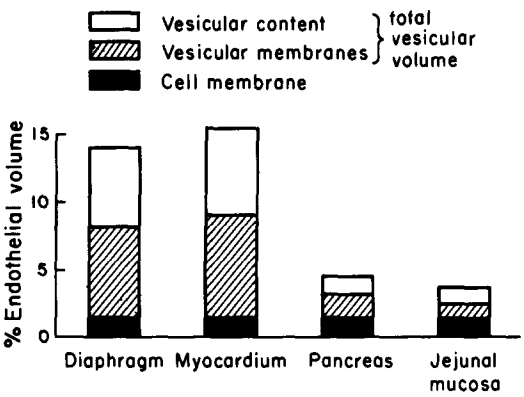

FIGURE 20 Fractional volumes occupied by the cell membrane and plasmalemmal vesicles in the peripheral zone of the endothelial cells. (Graph based on data given in Table VII.)

cysts. In our case the clusters in question may represent similar sites or early stages in fusion between the plasmalemma and the vesicle membranes.

Finally, our data show that although the four capillary beds examined belong to two distinct types of blood capillaries, there are consistent differences from one capillary bed to another concerning primarily the frequency of vesicles and fenestrae. The data suggest that there may be appreciable variation within each capillary type so that each vascular bed has a certain degree of structural specificity, in agreement with a number of physiological observations (41, 44–46).

We gratefully acknowledge the excellent technical assistance of Heide Plesken and Elizabeth Szabo.

This work was supported by Public Health Service Grant HE-05648.

Received for publication 19 June 1973, and in revised form 10 August 1973.

REFERENCES

1. BRUNS, R. R., and G. E. PALADE. 1968. Studies on blood capillaries. I. General organization of blood capillaries in muscle. *J. Cell Biol.* 37:244.
2. CLEMENTI, F., and G. E. PALADE. 1969. Intestinal capillaries. Permeability to peroxidase and ferritin. *J. Cell Biol.* 41:33.

3. PALADE, G. E. 1961. Blood capillaries of the heart and other organs. *Circulation.* **24**:368.
4. BRUNS, R. R., and G. E. PALADE. 1968. Studies on blood capillaries. II. Transport of ferritin molecules across the wall of muscle capillaries. *J. Cell Biol.* **37**:277.
5. CASLEY-SMITH, J. R. 1970. Endothelial fenestrae: their occurrence and permeabilities, and their probable physiological roles. Septième Congrès International de Microscopie Électronique, Grenoble. Société Française de Microscopie Electronique, Paris, France. **III**:49.
6. CASLEY-SMITH, J. R. 1970. The functioning of endothelial fenestrae on the arterial and venous limbs of capillaries, as indicated by the differing directions of passage of proteins. *Experientia.* **26**:852.
7. SIMIONESCU, N., M. SIMIONESCU, and G. E. PALADE. 1972. Permeability of intestinal capillaries. Pathway followed by dextrans and glycogens. *J. Cell Biol.* **53**:365.
8. SIMIONESCU, N., M. SIMIONESCU, and G. E. PALADE. 1973. Permeability of muscle capillaries to exogenous myoglobin. *J. Cell Biol.* **57**:424.
9. FERNANDO, N. V. P., and H. Z. MOVAT. 1964. The fine structure of the terminal vascular bed. III. The capillaries. *Exp. Mol. Pathol.* **3**:87.
10. WOLFF, J., and H. J. MERKER. 1966. Ultrastruktur und Bildung von Poren im Endothel von porösen und geschlossenen Kapillaren. *Z. Zellforsch. Mikrosk. Anat.* **73**:174.
11. WOLFF, J. 1966. Elektronenmikroskopische Untersuchungen über die Vesikulation im Kapillarendothel. Lokalisation, Variation und Fusion der Vesikel. *Z. Zellforsch. Mikrosk. Anat.* **73**:143.
12. RAYNS, D. G., F. O. SIMPSON, and W. S. BERTAUD. 1968. Surface features of striated muscle. I. Guinea-pig cardiac muscle. *J. Cell Sci.* **3**:467.
13. CASLEY-SMITH, J. R. 1969. The dimensions and numbers of small vesicles in cells, endothelial and mesothelial and the significance of these for endothelial permeability. *J. Microsc. (Oxf.).* **90**:251.
14. NICKEL, E., and E. GRIESHABER. 1969. Elektronenmikroskopische Darstellung der Muskelkapillaren im Gefrierärtzbild. *Z. Zellforsch. Mikrosk. Anat.* **95**:445.
15. FRIEDERICI, H. H. R. 1968. The tridimensional ultrastructure of fenestrated capillaries. *J. Ultrastruct. Res.* **23**:444.
16. FRIEDERICI, H. H. R. 1969. On the diaphragm across the fenestrae of capillary endothelium. *J. Ultrastruct. Res.* **27**:373.
17. WISSE, E. 1970. An electron microscopic study of the fenestrated endothelial lining of rat liver sinusoids. *J. Ultrastruct. Res.* **31**:125.
18. WEINSTEIN, R. S., and N. SCOTT MCNUTT. 1970. Electron microscopy of freeze-cleaved and etched capillaries. *In* Microcirculation, Perfusion, and Transplantation of Organs. Th. J. Malinin, B. S. Linn, A. B. Callahan, and W. D. Warren, editors. Academic Press, New York. 23.
19. LEAK, L. V. 1971. Frozen-fractured images of blood capillaries in heart tissue. *J. Ultrastruct. Res.* **35**:127.
20. MOOR, H., and K. MÜHLETHALER. 1963. Fine structure in frozen etched yeast cells. *J. Cell Biol.* **17**:609.
21. BRANTON, D. 1966. Fracture faces of frozen membranes. *Proc. Natl. Acad. Sci. U. S. A.* **55**:1048.
22. TILLACK, T. W., and V. T. MARCHESI. 1970. Demonstration of the outer surface of freeze-etched red blood cell membranes. *J. Cell Biol.* **45**:649.
23. RHODIN, J. A. G. 1962. The diaphragm of capillary endothelial fenestrations. *J. Ultrastruct. Res.* **6**:171.
24. MAUL, G. G. 1971. Structure and formation of pores in fenestrated capillaries. *J. Ultrastruct. Res.* **36**:768.
25. VENKATACHALAM, M. A., and M. J. KARNOVSKY. 1972. Extravascular protein in kidney. An ultrastructural study of its relation to renal peritubular capillary permability using protein tracers. *Lab. Invest.* **27**:435.
26. ALTSCHUL, R. 1954. Endothelium, its development, morphology, function and pathology. The Macmillan Company, New York. 7.
27. KROGH, A. 1959. The anatomy and physiology of capillaries. 3rd edition. Hafner Publishing Co., Inc., New York. 22 and 70.
28. FLOREY, H. W., J. C. F. POOLE, and G. A. MEEK. 1959. Endothelial cells and "cement" lines. *J. Pathol. Bacteriol.* **77**:625.
29. WIEDEMAN, M. P. 1963. Dimensions of blood vessels from distributing artery to collecting vein. *Circ. Res.* **12**:375.
30. FAWCETT, D. W. 1963. Comparative observations on the fine structure of blood capillaries. *In* The Peripheral Blood Vessels. T. L. Orbison and D. E. Smith, editors. The Williams & Wilkins Company, Baltimore. 17.
31. FUCHS, W. 1964. Elektronmikroskopische Untersuchungen menschlicher Muskelkapillaren bei Diabetes Mellitus. *Frankfurter. Z. Pathol.* **73**:318.
32. VRACKO, R. 1970. Skeletal muscle capillaries in nondiabetics. A quantitative analysis. *Circulation.* **41**:285.

33. LANDIS, E. M., and J. R. PAPPENHEIMER. 1963. Exchange of substance through the capillary walls. *In* Handbook of Physiology. W. F. Hamilton and P. Dow, editors. American Physiology Society, Washington, D. C. **II(2):** 961.
34. GROTTE, G. 1956. Passage of dextran molecules across the blood-lymph barrier. *Acta Chir. Scand. Suppl.* **211:**1.
35. KARNOVSKY, M. J. 1967. The ultrastructural basis of capillary permeability studied with peroxidase as a tracer. *J. Cell Biol.* **35:**213.
36. KARNOVSKY, M. J. 1970. Morphology of capillaries with special reference to muscle capillaries. *In* Capillary Permeability. Alfred Benzon Symposium II. C. Crone and N. A. Lassen, editors. Academic Press, Inc., New York. 341.
37. LASSEN, N. A., and J. TRAP-JENSEN. 1970. Estimation of the fraction of the inter-endothelial slit which must be open in order to account for the observed transcapillary exchange of small hydrophilic molecules in skeletal muscle in man. *In* Capillary permeability. Alfred Benzon Symposium II. C. Crone and N. A. Lassen, editors. Academic Press, Inc. New York. 647.
38. CASLEY-SMITH, J. R. 1963. The Brownian movements of pinocytotic vesicles. *J. R. Microsc. Soc.* **82:**257.
39. TOMLIN, S. G. 1969. Vesicular transport across endothelial cells. *Biochim. Biophys. Acta.* **183:**559.
40. SHEA, ST. M., and M. J. KARNOVSKY. 1969. Vesicular transport across endothelium: simulation of a diffusion model. *J. Theor. Biol.* **24:**30.
41. RENKIN, E. M. 1964. Transport of large molecules across capillary walls. *Physiologist.* **7:**13.
42. SATIR, B., C. SCHOOLEY, and P. SATIR. 1972. Membrane reorganization during secretion in *Tetrahymena*. *Nature* (*Lond.*). **235:**53.
43. SATIR, B., C. SCHOOLEY, and P. SATIR. 1973. Membrane fusion in a model system. Mucocyst secretion in *Tetrahymena*. *J. Cell Biol.* **56:**153.
44. POLOSA, C., and W. F. HAMILTON. 1963. Blood volume and intravascular hematocrit in different vascular beds. *Am. J. Physiol.* **204:** 903.
45. RENKIN, E. M. 1967. Blood flow and transcapillary exchange in skeletal and cardiac muscle. *In* International Symposium on the Coronary Circulation and Energetics of the Myocardium. G. Marchetti and B. Taccardi, editors. Karger, Basel/New York.
46. FOLKOW, B., and E. NEIL. 1971. Circulation. Oxford University Press, New York.
47. SMITH, U., J. W. RYAN, and D. S. SMITH. 1973. Freeze-etch studies of the plasma membrane of pulmonary endothelial cells. *J. Cell Biol.* **56:**492.